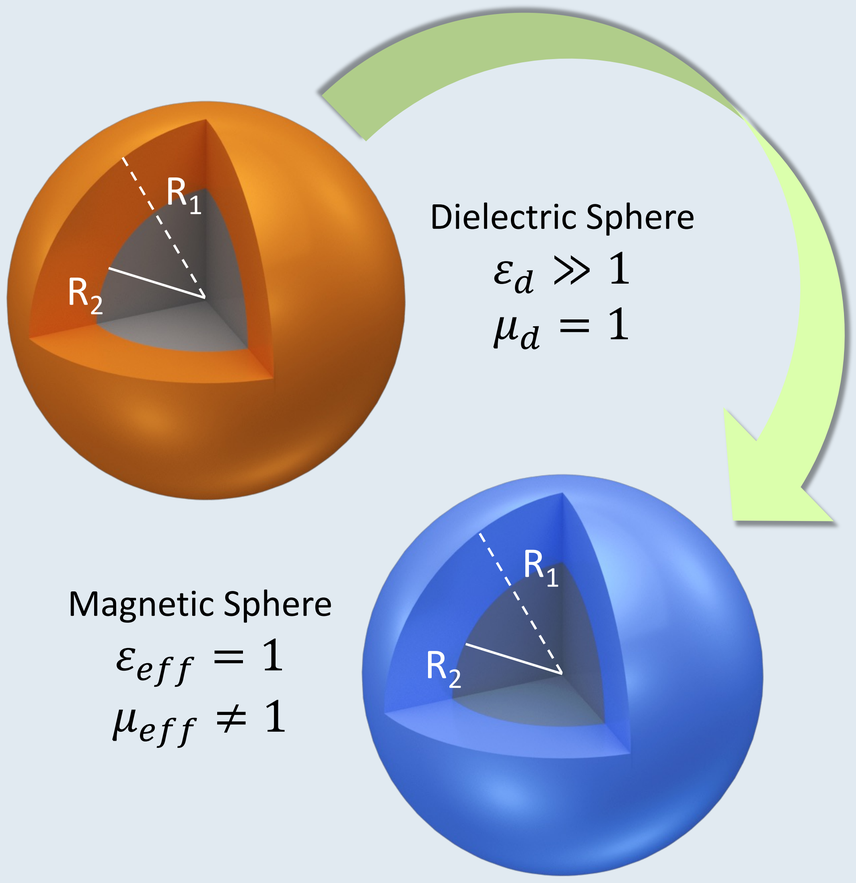

Artificial Magnetism Obtained Through Mie Resonances In High-Index Hollow Spheres

A different approach to Artificial Magnetism revisiting the standard plane-wave scattering towards spherical particles (i.e. Mie Theory).

A. Contestabile[1] , G. Castaldi[2], V. Galdi[2], A. Galante[3], M. Alecci[3], D.Burov[1], C. Rizza[1]
1. University of L'Aquila, Department of Physical and Chemical Sciences, L'Aquila, Italy.
2. University of Sannio, Department of Engineering, Fields & Waves Lab, Benevento, Italy.
3. University of L'Aquila, Department of Life, Health Environmental Sciences, L'Aquila, Italy.

Abstract

The pursuit of artificial magnetism within metamaterials research has long been a focal point. Traditional methods rely on analyzing complex configurations such as arrays of subwavelength particles or split-rings, but unfortunately, they fail at subwavelength scales. Revisiting Mie theory we have already demonstrated that a high-index dielectric sphere accurately replicates the external near-field characteristics of a negative-permeability sphere at its lowest Mie resonance frequency [1].

Furthermore, for subwavelength spheres (R_1=30 mm) with permittivity within the range of 10^3 to 10^5, the resulting magnetic sphere exhibits an effective permeability close to -2 [2]. Here we focus on near-field operations, showing that a high-index hollow sphere at Mie resonance can accurately sustain an external near-field pattern resembling that of an arbitrary negative-permeability hollow sphere of equivalent dimensions.

Methodology

To carry out our analysis we set our COMSOL Multiphysics® package [3] in the RF Module, choosing the default frequency-domain study. The EM field is excited using a non-resonant loop coil, modeled as an Integral-type Boundary Probe. We exploited the setup's z-axis rotational invariance to perform 2D full-wave simulations in cylindrical coordinates (r, z).

Operatively, at the lowest Mie resonance frequency ($f_{res} \propto 10^2$ MHz), we investigated the scattering from the equivalent magnetic hollow sphere by performing a parametric sweep of the negative magnetic permeability μ_{eff}, in order to find the value of μ_{eff} that accurately reproduces the field distribution outside the sphere.

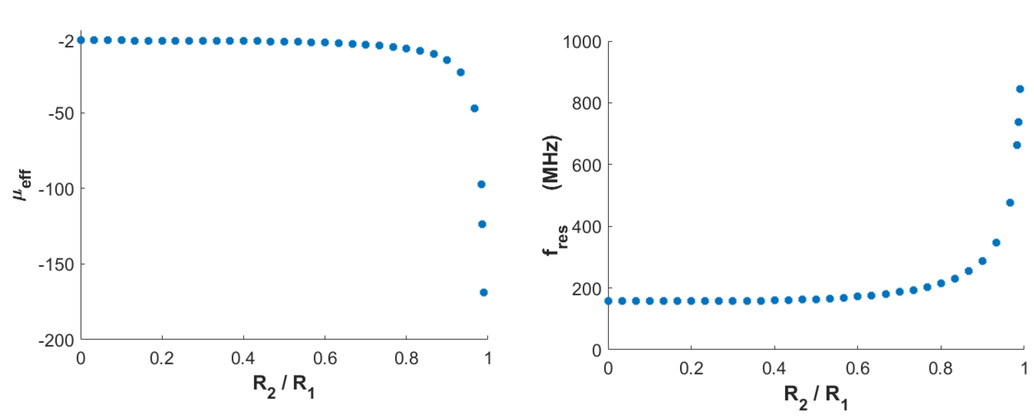

FIGURE 1. Left: behavior of μ_{eff} w.r.t. the normalized cavity radius R_2 / R_1. Right: behavior of the L=1 mode resonance frequency.

Results

In Figure 1, we plot μ_{eff} as a function of the normalized cavity radius R_2/R_1. As expected, the effective permeability is $\mu_{eff} \approx -2$ when $R_2 = 0$, whereas, by increasing the cavity radius R_2, μ_{eff} spans up to values of the order of -10^2.

In addition, in Figure 2, we report, for both the spheres, the absolute value of the magnetic field along the z-axis for R_2 = 0, 20, 25 mm, respectively. These results provide numerical evidence that the dielectric hollow sphere accurately reproduces the scattered magnetic field of the electromagnetic configuration with negative permeability in the region outside the sphere (i.e., for z > R_1).

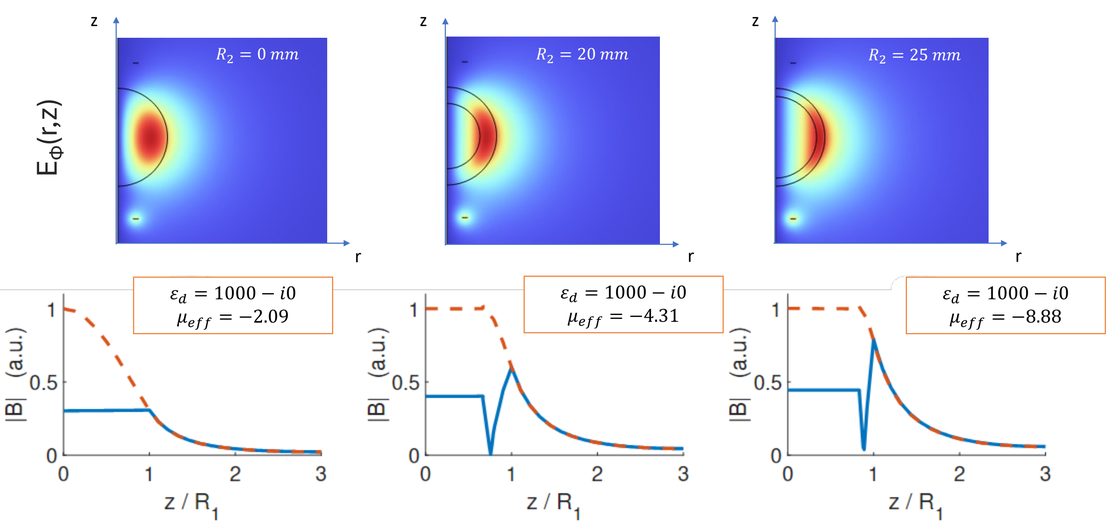

FIGURE 2. Electric (up) and magnetic (down) field distributions for R_2 = 0, 20, 25 mm. The Dielectric Sphere magnetic field profile (red) is compared to the one of the equivalent magnetic sphere (blue).

REFERENCES

1. C. Rizza et al. , "Theory of spoof magnetic localized surface plasmons beyond effective medium approximations", J. Phys. D: Appl. Phys., 54, 165108, 2021.
2. C. Rizza et al. , "Artificial Magnetism through Mimicking Magnetic Localized Surface Plasmons" Phys. Rev. Applied, 12, 044023, 2019.
3. COMSOL Multiphysics (COMSOL AB, Stockholm, Sweden).

UNIVERSITÀ DEGLI STUDI DELL'AQUILA
DSFC Dipartimento di Scienze Fisiche e Chimiche
DEPARTMENT OF LIFE, HEALTH & ENVIRONMENTAL SCIENCES
Finanziato dall'Unione europea NextGenerationEU
Ministero dell'Università e della Ricerca
Italiadomani PIANO NAZIONALE DI RIPRESA E RESILIENZA
GAMING

Excerpt from the Proceedings of the COMSOL Conference 2024 Florence

Guidelines

General Notes for Using the Template

- Do not adjust the template; work within it. See the examples provided.
- Left align text within textboxes, and do not justify your text.
- Titles are the largest font on the slide (90–120 pt.), then subtitles (70–80 pt.). Captions, references, and affiliation are the smallest text (18–40 pt.).
- Titles and subtitles are bold; any other use of bold should be for emphasis.
- Text is either black or grey and should only be adjusted for diagrams.
- Images can be adjusted and fitted into the boxes using the *Crop* feature. (In PowerPoint: *Format* tab → *Size* section on the right → *Crop*.)

Please keep in mind:

- **The solid red lines are the 3 mm that will be cut off during printing.**
- The dotted lines represent a small margin that may or may not be cut off during printing.

Exporting an Image for the Header

The settings shown on the right export the highest quality image with a transparent background.

The most important settings to use are the two outlined in pink. This will export an image that can be placed in the blue space of the header.

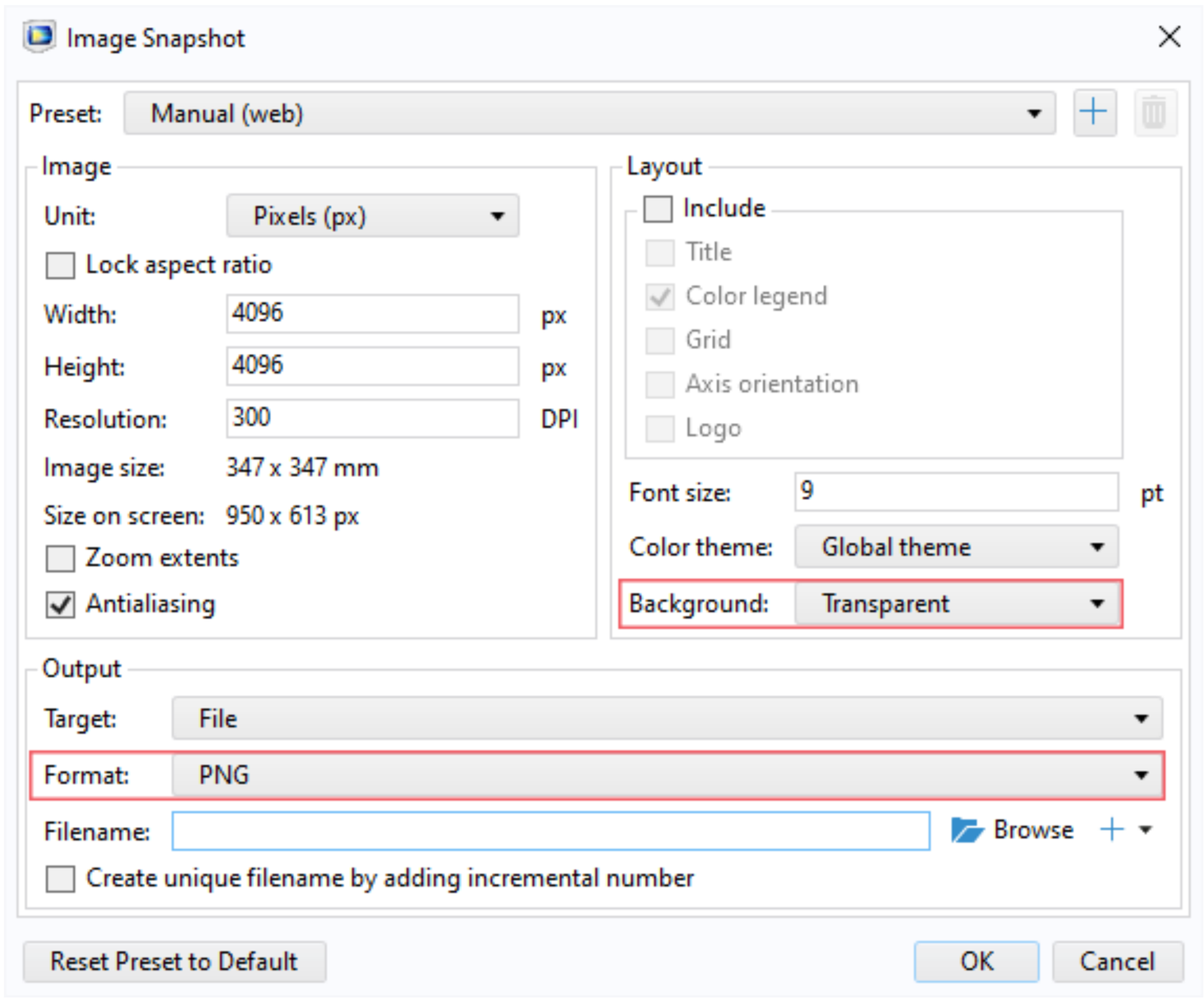

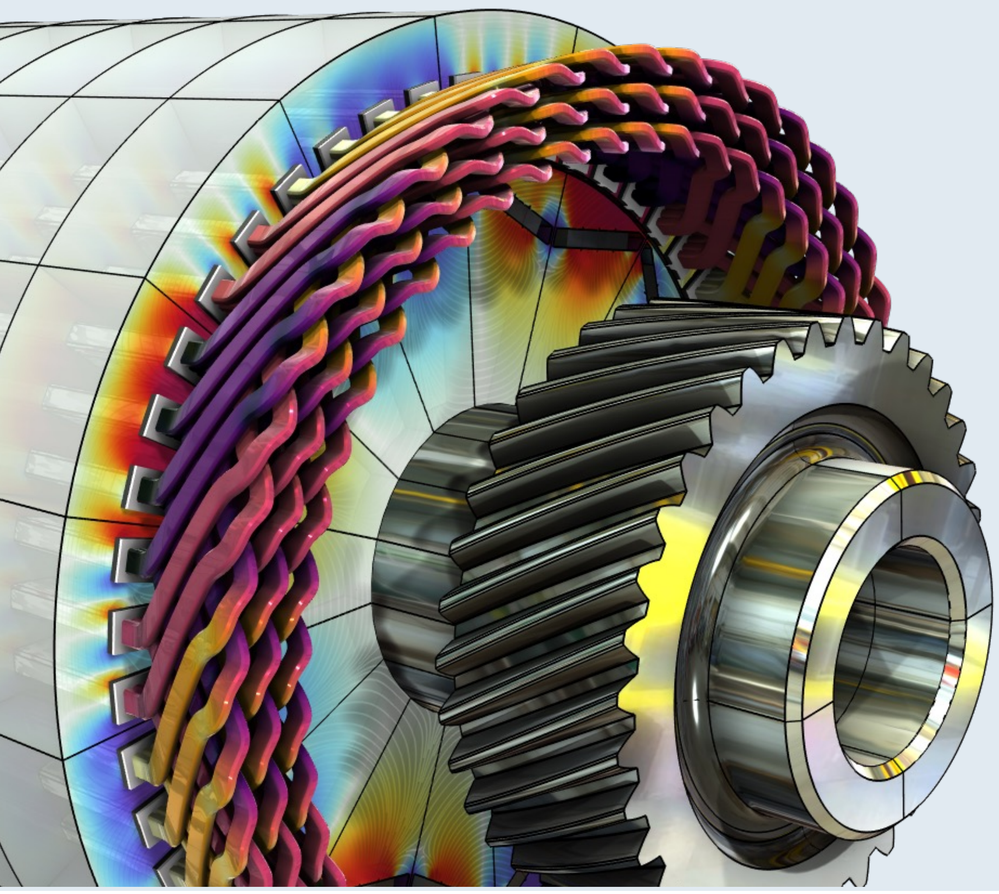

Analysis of a Permanent Magnet Motor in 3D

Optimize permanent magnet (PM) motor performance by understanding their full behavior, including sensitivity to high temperatures.

J. A. Smith[1], M. B. Smith[2]
1. Department (if applicable), Organization, City, Country.
2. Department (if applicable), Organization, City, Country.

Abstract

While PM motors are valued for the energy savings that they provide, there are some design limitations to address. For example, permanent magnets are sensitive to high temperatures. Such temperatures can occur when currents, particularly eddy currents, generate heat losses.

The findings offer greater insight into the behavior of PM motors, particularly by capturing the eddy current losses that occur within the magnets. This information serves as a useful resource for improving the design of PM motors, and therefore the technology they help power.

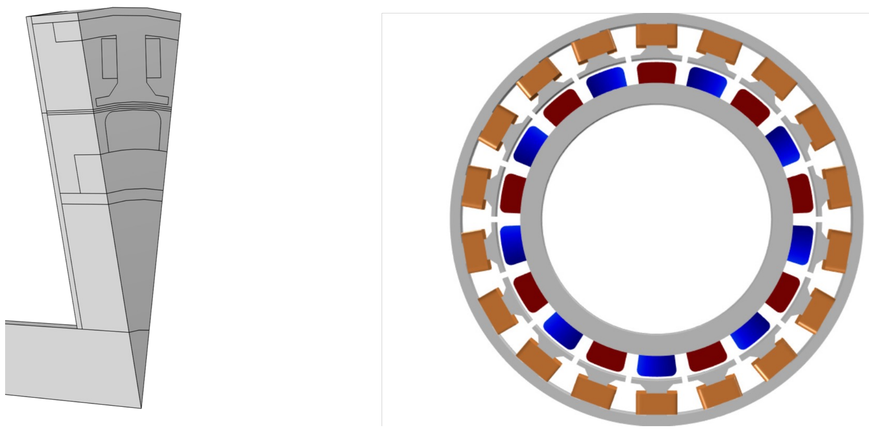

FIGURE 1. Left: Permanent motor sector. Right: Drawing of the PM motor.

Methodology

An 18-pole PM motor is modeled in 3D. Sector symmetry and axial mirror symmetry are utilized to reduce the computational effort while capturing the full 3D behavior of the device.

The conducting part of the rotor is modeled using Ampère's law:

$$\sigma\frac{\delta \boldsymbol{A}}{\delta t}+\nabla\times\left(\frac{1}{\mu}\nabla\times\boldsymbol{A}\right)=0$$

Results

The results can be seen in Figure 2, which shows the magnetic flux density for the motor in it's stationary state, that is, the initial conditions for the time-dependent simulation. In this state, the coil current is zero. It also shows the magnetic flux density for the motor after revolving one sector angle. In this plot, the air and coil domains are excluded in order to get a better view.

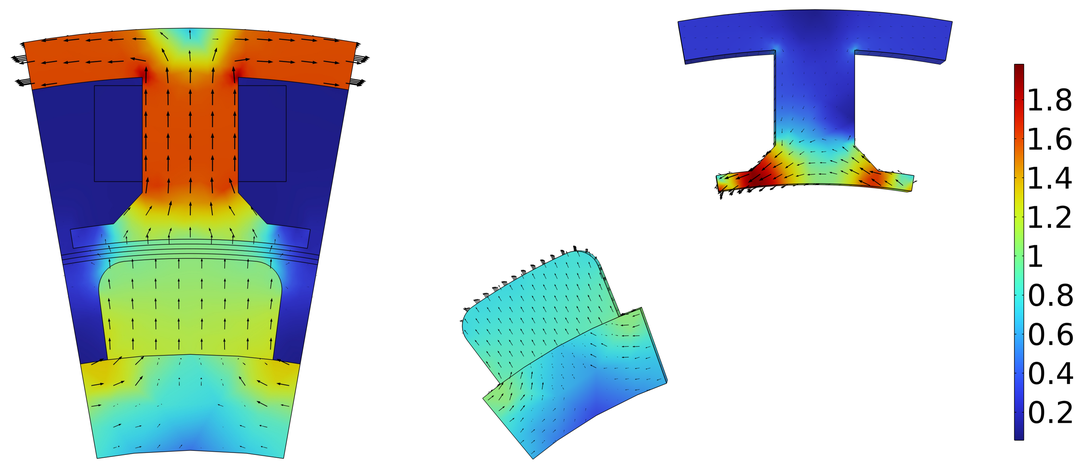

FIGURE 2. Left: Magnetic flux density from the permanent magnets with only the rotor at rest. Right: Magnetic flux density after revolving one sector angle.

REFERENCES

1. Author first initial and last name, "Article Title", *Journal*, Volume (vol.), Page numbers (pp.), Year.
2. Author first initial and last name, "Article Title", *Journal*, Volume (vol.), Page numbers (pp.), Year.
3. Author first initial and last name, "Article Title", *Journal*, Volume (vol.), Page numbers (pp.), Year.

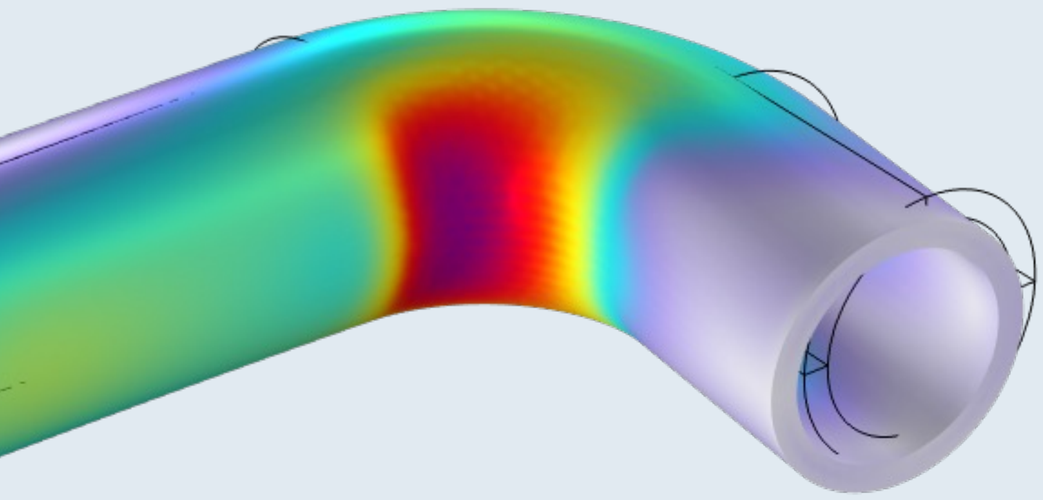

The Intriguing Stresses in Pipe Bends

For many structural engineers, beam theory is a popular analysis tool. Using the equations can be beneficial when considering structural behavior, as they are easy to apply and provide useful results. This work investigates one such case.

J. A. Smith[1], M. B. Smith[2]

1. Department (if applicable), Organization, City, Country.
2. Department (if applicable), Organization, City, Country.

Introduction & Goals

Pipe bends are common in piping systems, which typically transport liquids or gas, often under high pressure. One place where you may find a lot of pipes are oil tankers. The labyrinthine piping systems can look pretty fascinating.

Many piping standards (or codes) used for industrial applications are based on beam theory when it comes to the structural analysis. But, as we have already discovered, pipe bends generally do not behave like beams. When digging into piping standards, you will find a lot of information dedicated to pipe bends. In particular, piping standards recommend to apply correction factors to the stiffness and stresses for curved pipe sections. (Ref. 1)

FIGURE 1. Piping systems on an oil/chemical tanker. Image licensed under CC BY-SA 3.0 via Wikimedia Commons.

Methodology

The pipe is slender with a constant cross section, so it would seem like a natural choice to treat such a structure as a beam in a simplified analysis. The bending moment is the only load acting on the structure, and it's thus constant for any given section along the entire beam axis.

The maximum stress even occurs on the *inside* of the pipe. The cross section of the bend also deforms significantly, and, more specifically, it ovalizes with the major axis either being oriented in the bend plane or perpendicular to it depending on the direction of the bending moment.

Results

At a relative thickness of $t/R_o \approx 35\%$ (which for any real application would be considered very thick), the stress distribution starts to change quite significantly. Additional perpendicular tensional stresses superpose the beam solution at the inner- and outer-bend radii.

Simultaneously, the top and bottom of the pipe show compressional stresses. These additional circumferential stresses arise due to the ovalization of the cross section. Ordinary beam theory explicitly ignores such cross-sectional deformations, and it does fall short in capturing its effect.

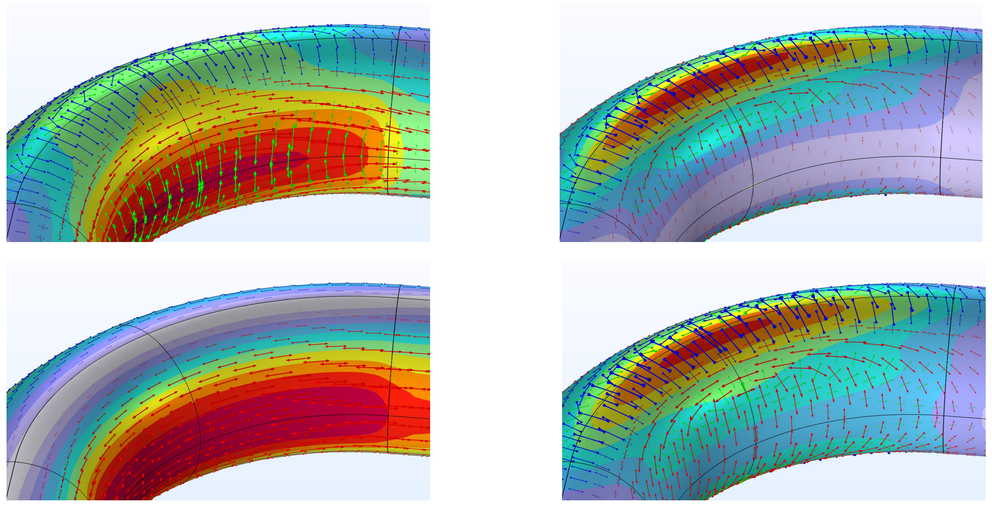

FIGURE 2. View of the pipe bend showing the von Mises stress (normalized) and principal stresses for different wall thicknesses.

REFERENCES

1. E.A. Wais and E.C. Rodabaugh, "Background of SIFs and Stress Indices for Moment Loadings of Piping Components", United States, 2005; https://www.osti.gov/biblio/841246
2. "Stress Intensification Factors (i-Factors), Flexibility Factors (k-Factors), and Their Determination for Metallic Piping Components", ASME, 2017; https://www.asme.org/codes-standards/find-codes-standards/b31j-stress-intensification-factors-flexibility-factors-determination-metallic-piping-components/2017/drm-enabled-pdf

- In order to carry out our analysis we set our COMSOL Multiphysics package [4] in the RF module, choosing the default frequency-domain study. The electromagnetic field is excited using a non-resonant loop coil, modeled as an Integral-type Boundary Probe. We exploited the setup's z-axis rotational invariance to perform 2D full-wave simulations in cylindrical coordinates (r, z).

- The exciting loop-coil has zero thickness along the z-axis and a constant surface current density only along the azimuthal component. The computational domain is delimited by scattering boundary conditions (spherical-waves type). Finally, we adopted the user-controlled mesh calibrated for General Physics of the predefined extra-fine free triangular type.